



1 **Tracer-based investigation of organic aerosols in marine**
2 **atmospheres from marginal seas of China to the northwest**
3 **Pacific Ocean**

4 Tianfeng Guo¹, Zhigang Guo¹, Juntao Wang², Jialiang Feng^{3*}, Huiwang Gao^{2,4}, Xiaohong
5 Yao^{2,4*}

6 ¹ Shanghai Key Laboratory of Atmospheric Particle Pollution and Prevention, Department of Environmental
7 Science and Engineering, Fudan University, Shanghai 200433, China;

8 ² Lab of Marine Environmental Science and Ecology, Ministry of Education, Ocean University of China,
9 Qingdao 266100, China

10 ³ School of Environmental and Chemical Engineering, Shanghai University, Shanghai 200444, China

11 ⁴ Pilot National Laboratory for Marine Science and Technology (Qingdao), Qingdao, China

12 *Correspondence to:* Xiaohong Yao (xhyao@ouc.edu.cn); Jialiang Feng (fengjialiang@shu.edu.cn)

13

14 **Abstract.** We investigated the geographic distributions of organic tracers in total suspended particles over
15 marginal seas of China, including the Yellow and Bohai seas (YBS) and the South China Sea (SCS), and the
16 northwest Pacific Ocean (NWPO) in spring, when Asian outflows strongly affect downwind marine
17 atmospheres. The comparison of levoglucosan observed in this study with values from the literature implied that
18 the contribution from biomass burning emissions to marine aerosols over the NWPO may have increased largely
19 over the last decades. The increase led to the mean value of levoglucosan ($8.2 \pm 14 \text{ ng m}^{-3}$) observed over the
20 NWPO closer to that over the SCS and almost half of that over the YBS. Small geographic differences in
21 monoterpene-derived and sesquiterpene-derived secondary organic tracer concentrations were obtained among
22 the three atmospheres, although the causes may differ. By contrast, a large difference in isoprene-derived
23 secondary organic tracer concentrations was observed among the three atmospheres, with the sum of tracer
24 concentrations over the SCS ($45 \pm 54 \text{ ng/m}^3$) several times and approximately one order of magnitude greater
25 than that over the YBS ($15 \pm 16 \text{ ng/m}^3$) and the NWPO ($2.3 \pm 1.6 \text{ ng/m}^3$), respectively. The geographic distribution
26 of aromatic-derived secondary organic tracers was similar to that of isoprene-derived secondary organic tracers,
27 with a slightly narrower difference, i.e., $1.8 \pm 1.7 \text{ ng/m}^3$, $1.1 \pm 1.4 \text{ ng/m}^3$ and $0.3 \pm 0.5 \text{ ng/m}^3$ over the SCS, the YBS
28 and the NWPO, respectively. We discuss the causes of the distinctive geographic distributions of these tracers
29 and present the tracer-based estimation of organic carbon.

30 **1 Introduction**

31 Aerosols that emanate from biomass burning (BB) consist primarily of carbonaceous components and inorganic
32 salts, which can affect the climate directly by absorbing solar radiation or indirectly by acting as either cloud
33 condensation nuclei (CCN) or ice nuclei (IN) (Bougiatioti et al., 2016; Chen et al., 2017; Hsiao et al., 2016).
34 High BB aerosol emissions zones include boreal forests (e.g., in Eurasia and North America), tropical forests
35 (e.g., in southeast Asia and the tropical Americas), and agriculture areas where crop residuals are burned (e.g., in
36 developing countries such as China and India, etc.) (van der Werf et al., 2006). BB aerosols can undergo
37 long-range transport in the atmosphere, which can carry them from the continents to the oceans (Ding et al.,
38 2013; Fu et al., 2011; Kanakidou et al., 2005). For example, BB aerosols from boreal forest wildfires in Russia



39 and China reportedly made an appreciable contribution to atmospheric particle loads observed over the Arctic
40 Ocean and northwestern Pacific Ocean (NWPO) based on specific tracers of BB (Ding et al., 2013). Although
41 open wildfires from forests occur sporadically in terms of strength and occurrence frequency, global warming
42 could be conducive to vegetation fires (Running, 2006) and thus increase emissions of BB aerosols. In this
43 century, nine years were among the ten hottest global years on record, with 2014–2018 being ranked as the top
44 five hottest years (<https://www.climatecentral.org/gallery/graphics/the-10-hottest-global-years-on-record>). The
45 question is automatically raised: how do BB aerosols in the marine atmosphere in the hottest global years
46 change against those observations previously reported?

47 In addition to BB aerosols, secondary oxidation of biogenic volatile organic compounds (BVOCs) and
48 anthropogenic VOCs (AVOCs) also contribute to the particulate carbonaceous components of marine
49 atmospheres (Kanakidou et al., 2005). Many field and modeling studies have proposed that secondary organic
50 aerosols (SOAs) arising from the oxidation of phytoplankton-derived isoprene may affect the chemical
51 composition of marine atmospheric aerosols and consequently impact CCN loading and cloud droplet number
52 concentrations (Ekström et al., 2009; Meskhidze and Nenes, 2006; Claeys et al., 2004). Several modeling
53 studies have shown that the NWPO may experience the greatest increases in sea surface temperature and CO₂
54 input under a future warming climate in the future (John et al., 2015; Lauvset et al., 2017). The Kuroshio
55 Extension current system leads the NWPO to be an active subtropical cyclone basin, promoting biogenic
56 activities (Hu et al., 2018). From the perspective of global change, it is a long-term need to study the dynamic
57 changes in atmospheric aerosols derived from marine sources over the NWPO and adjacent marginal seas of
58 China, as well as their potential effects on climate.

59 Not limited by phytoplankton-derived isoprene, BVOCs emitted from continental ecosystems and their
60 oxidation products can also affect the atmosphere in remote marine areas through long-range transport (Hu et al.,
61 2013a; Ding et al., 2013; Kang et al., 2018; Fu et al., 2011; Kawamura et al., 2017). BVOCs consist primarily of
62 isoprene, monoterpenes, sesquiterpenes, and their oxygenated hydrocarbons such as alcohols, aldehydes, and
63 ketones (Guenther et al., 2006; Ehn et al., 2014) and account for the majority of the global VOC inventory (Zhu
64 et al., 2016a, b; Heald et al., 2008). However, emissions fluxes and oxidation processes of BVOCs show great
65 variation, depending on global warming and other factors such as regional landscape, other pollutants in the
66 ambient air etc. (Ait-Helal et al., 2014; Hu and Yu, 2013; Peñuelas and Staudt, 2010). Unlike a potential
67 increase in BVOC-derived organics aerosols in marine atmospheres under global warming, anthropogenic
68 VOCs and carbonaceous particles over the continents have been decreased because of effective mitigation of air
69 pollutants in the last decades (Sharma, 2004; Murphy et al., 2011; Zhang et al., 2012). In the northern
70 hemisphere, marine atmospheres are also usually affected by anthropogenic pollutants to some extent, most of
71 which are derived from long-range transport from continents (Kang et al., 2019; Bao et al., 2018; Zhang et al.,
72 2017). The reverse trends in BVOC and anthropogenic VOC would change the composition, sources of
73 carbonaceous particles in marine atmospheres. Update observations are thereby needed to reveal the change and
74 service the future study of the impacts.

75 In this study, we analyzed the concentrations of some typical organic tracers in aerosol samples obtained from
76 three cruise campaigns from the marginal seas of China, including in the South China Sea (SCS) in 2017,
77 Yellow Sea and Bohai Sea (YBS), to the NWPO in 2014, both in springtime. We investigated the influences of
78 BB aerosols from continents over three marine atmospheres, quantified the contributions of various precursors
79 to the observed SOA in marine atmospheres using organic tracers established in the literature, and explored the
80 formation pathways of SOA from their precursors during long-range transport in these hottest global years.
81 Particularly, we conducted a comprehensive comparison of this observation with those reported in literature in
82 terms of long-term variations and geographic distributions of these tracers, etc.



83 2 Materials and Methods

84 Total suspended particulate (TSP) samples were collected over the NWPO from 19 March to 21 April 2014,
85 over the YBS from 30 April to 17 May 2014, and over the SCS from 29 March to 4 May 2017. All samples were
86 collected on the upper deck of the R/V Dong Fang Hong II, which sits ~8 m above the sea surface. To avoid
87 contamination from the ship's exhaust, samples were collected only when the ship was sailing, and the wind
88 direction ranged from -90° to 90° relative to the bow. TSP samples were collected on quartz fiber filters
89 (Whatman QM-A) that had been pre-baked for 4 h at 500°C prior to sampling using a high-volume sampler
90 (KC-1000, Qingdao Laoshan Electric Inc., China). The sampling duration was 15–20 h at a flow rate of ~ 1000 L
91 /min. After sampling, the sample filters were wrapped in baked aluminum foil and sealed in polyethylene bags,
92 then stored at -20°C and transported to the laboratory. Field blanks were collected during each sampling period.
93 However, one sampler was out of service during the cruise on the SCS. As a compromise, cellulose filters
94 (Whatman 41) previously intended for elemental analyses were used for analyses of the organic tracers in TSP.
95 The method for determining the concentrations of tracers was adapted from Kleindienst et al. (2007) and Feng et
96 al. (2013). Briefly, 20 mL dichloromethane/methanol (1:1, v/v) was used for ultrasonic extraction of 40 cm² of
97 each filter at room temperature three times. The combined extracts were filtered, dried under a gentle stream of
98 ultrapure nitrogen, and then derivatized with 100 μL N,O-bis-(trimethylsilyl)-trifluoroacetamide (BSTFA,
99 containing 1% trimethylchlorosilane as a catalyst) and 20 μL pyridine at 75°C for 45 min. Gas chromatography
100 mass spectrometry (GC-MS) analyses were conducted with an Agilent 6890 GC/5975 MSD. Prior to solvent
101 extraction, methyl- β -D-xylanopyranoside (MXP) was spiked into the samples as an internal/recovery standard.
102 Hexamethylbenzene was added prior to injection as an internal standard to check the recovery of the surrogates.
103 Like those reported by Feng et al. (2013), the primary organic tracers analyzed in this study included
104 levoglucosan (LEVO), mannosan, and galactosan. Four types of secondary organic tracers were used:
105 isoprene-derived secondary organic tracers (SOA_I) including 2-methylglyceric acid (2-MGA), C5-alkene triols
106 (cis-2-methyl-1,3,4-trihydroxy-1-butene, 3-methyl-2,3,4-trihydroxy-1-butene and
107 trans-2-methyl-1,3,4-trihydroxy-1-butene), and MTLs (2-methylthreitol and 2-methylerythritol);
108 monoterpene-derived secondary organic tracers (SOA_M) including 3-hydroxyglutaric acid (HGA),
109 3-hydroxy-4,4-dimethylglutaric acid (HDMGA), and 3-methyl-1,2,3-butanetricarboxylic acid (MTBCA); the
110 sesquiterpene-derived secondary organic tracer (SOA_S) β -caryophyllinic acid; and the aromatic
111 (toluene)-derived secondary organic tracer (SOA_A) 2,3-dihydroxy-4-oxopentanoic acid (DHOPA). LEVO was
112 quantified based on authentic standards in this study. While the SOA tracers without available commercial
113 standards were quantified using methyl- β -D-xylanopyranoside (MXP) as a surrogate. To reduce the uncertainty
114 of quantification, relative response factors of the target tracers to MXP were estimated by comparing the area
115 ratio of typical target ions to MXP to that of total ions in selected samples that showed high concentrations of
116 the target tracers (Feng et al., 2013).

117 Field blanks and laboratory blanks (run every 10 samples) were extracted and analyzed in the same manner as
118 the ambient samples. Target compounds were nearly always below the detection limit in field and laboratory
119 blanks. Recoveries of the surrogate (MXP) were in the range of 70–110%. The reported results were corrected
120 for recovery, assuming that the target compounds had the same recovery as the surrogate. Duplicate analyses
121 indicated that the deviation was less than 15%.

122 However, the substitution of cellulose filters (Whatman 41) during the cruise on the SCS led to increased field
123 blank values for some tracers. The tracer concentrations in those samples were, however, over three times higher
124 than the field blank values, except for those of mannosan and galactosan. Data for mannosan and galactosan
125 were thus not available, nor were the total organic carbon concentrations, for samples collected during the cruise



126 on the SCS.

127 The concentrations of organic carbon (OC) and element carbon (EC) in each sample were analyzed with a DRI
128 2001A thermal/optical carbon analyzer (Atmoslytic Inc., Calabasas, CA, USA) using the IMPROVE
129 temperature program (Wang et al., 2015).

130 3. Results and Discussion

131 3.1 Spatiotemporal distributions of LEVO

132 Levoglucosan, mannosan, and galactosan produced by the pyrolysis of cellulose and hemicellulose have been
133 widely used as organic tracers of BB aerosols in ambient air (Ding et al., 2013; Fu et al., 2011; Feng et al.,
134 2013). The mean levels of LEVO in TSP collected during the cruises on the NWPO and the SCS were
135 comparable, at 8.2 ng/m³ and 9.6 ng/m³, respectively (Figure S1, Table 1). They were almost half of the mean
136 value of 21 ng/m³ during the cruise on the YBS, where high concentrations of BB aerosols have been observed
137 in continental atmospheres upwind of the YBS mainly from wildfires and the burning of burning crop residue,
138 wildfire, etc. (Yang et al., 2014; Feng et al., 2012; Feng et al., 2013). Unlike the smaller difference among the
139 means values, the concentration of LEVO fluctuated greatly among TSP samples in each oceanic zone, ranging
140 from 0.5 to 65 ng/m³ over the NWPO, from 1.0 to 30 ng/m³ over the SCS and from 2.5 to 42 ng/m³ over the
141 YBS (Fig. S1). High spatiotemporal variation in LEVO in TSP has also been observed in literature, with
142 concentrations of LEVO fluctuating around 0.2–41 ng/m³ during Arctic to Antarctic cruises from July to
143 September 2008 and from November 2009 to April 2010 (Hu et al., 2013b). Hu et al. (2013b) also reported the
144 highest LEVO concentrations occurring at mid-latitudes (30°–60° N and S) and the lowest at Antarctic and
145 equatorial latitudes over the several months of sampling. This distinctive geographical distribution was not
146 observed in the present study, as there were no significant differences in LEVO in TSP between the SCS and
147 NWPO ($P > 0.05$).

148 Narrow spatiotemporal variation in LEVO in TSP has been reported during summer sampling over the North
149 Pacific Ocean and the Arctic in 2003, with maximum and mean values as low as 2.1 ng/m³ and 0.5 ng/m³,
150 respectively (Ding et al., 2013). A lower mean value of LEVO of 1.0 ng/m³ has also been reported in the spring
151 over the island of Chichi-jima from 2001 to 2004 (Mochida et al., 2010), while the levels increased to 3.1 ± 3.7
152 ng/m³ in TSP collected on the island of Okinawa in 2009–2012 (Zhu et al., 2015). Using these previous
153 observations as a reference, our observations suggested that the contribution of BB aerosols to particle loading
154 over the NWPO may have increased continuously and largely over the last decades.

155 Due to the lack of BB sources in oceans, large spatiotemporal variation in the concentrations of LEVO in the
156 marine atmosphere may be related to the long-range transport of atmospheric particles from continents. Thus, 72
157 h back trajectories of air masses at a height of 1000 m during our sampling periods (Figs. 1, 2) were calculated
158 using the HYSPLIT model (<https://ready.arl.noaa.gov/HYSPLIT>). Based on the calculated back trajectories, TSP
159 samples could be classified into two categories with Category 1 representing continent-derived aerosol samples
160 and Category 2 being ocean-derived aerosol samples. All 12 samples collected over the YBS fell into Category 1
161 (Fig. 2). Half (11/19) of the samples collected over the NWPO were classified into Category 1 (Fig. 1). A
162 significant difference ($p < 0.05$) was obtained between the concentrations of LEVO in Category 1 (13 ± 18 ng/m³)
163 and Category 2 (2.0 ± 1.8 ng/m³) samples over the NWPO. The values in Category 2 were closer to the
164 springtime observations reported by Mochida et al. (2010) and Zhu et al. (2015) as well as the summer
165 observations reported by Ding et al. (2013), reflecting the marine background value less affected by continental
166 air masses. On the other hand, the much higher values in Category 1 than Category 2 further indicated a large

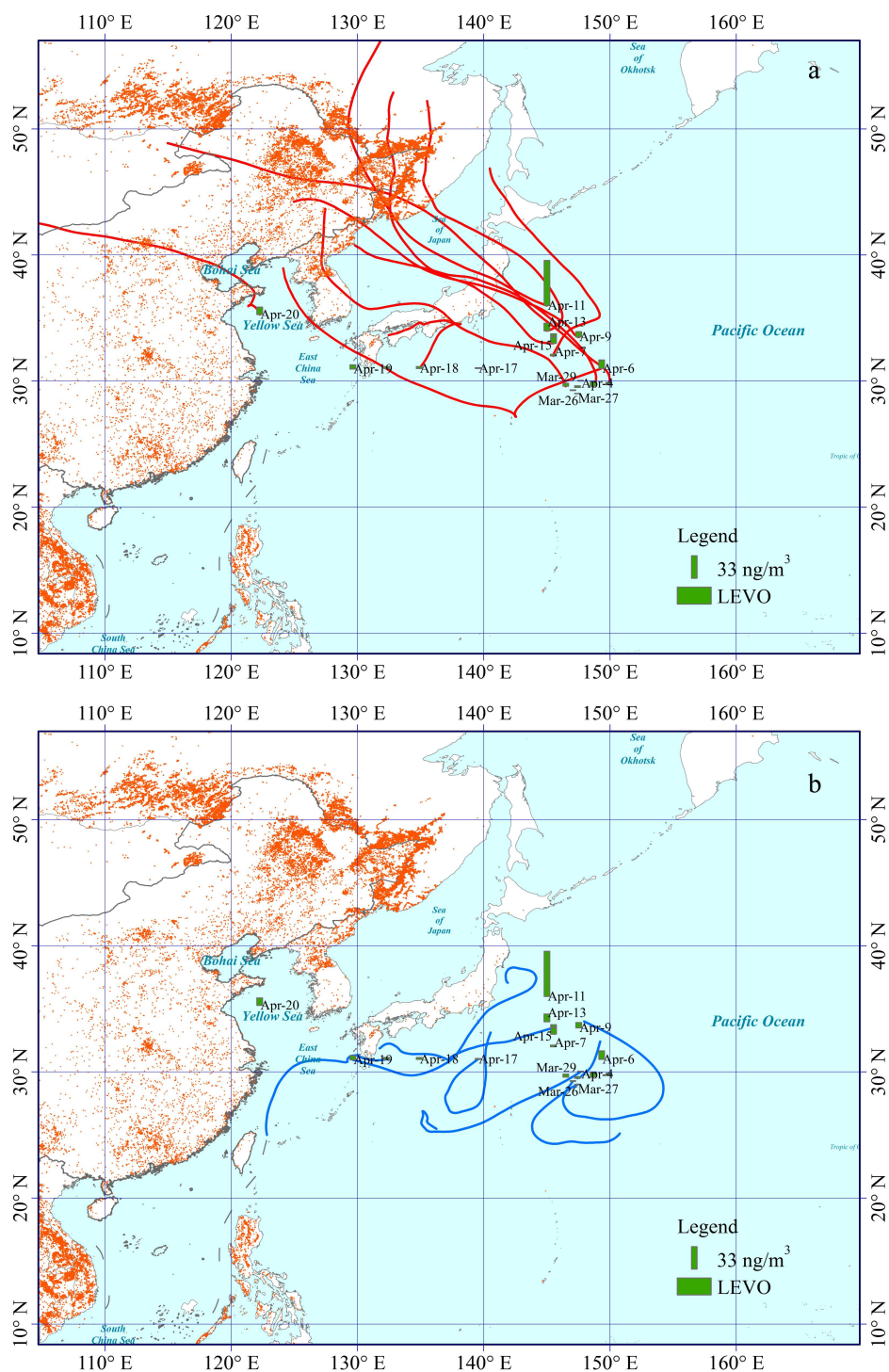


167 increase in contribution of BB aerosols being transported from the continents to the remote marine atmosphere
168 in 2014.

169 On 11 April 2014 over the NWPO, an episode of high LEVO concentration of 65 ng/m^3 occurred (Fig. 1). Like
170 LEVO, the concentrations of galactosan and mannosan in the sample were also the highest among all samples
171 collected over the NWPO. This sample was collected in the oceanic zone, approximately 500 km from the
172 continent of Japan. A combination of air mass back tracers and NASA's FIRMS Fire Map indicated strong BB
173 aerosol emissions from intense fire events in Siberia, followed by long-range transport with the westerly wind as
174 the major contributors to this anomaly (Fig. 1). A similar episodic concentration of LEVO of 27 ng/m^3 in TSP
175 was observed once previously over the NWPO during a circumnavigation cruise (Fu et al., 2011). By combining
176 satellite data with other observations, many studies in literature have found that BB aerosols from major forest
177 fires and smoke events in Siberia could be transported downwind to remote marine regions not only in spring,
178 but also in summer (Generoso et al., 2007; Ding et al., 2013; Huang et al., 2009). In a few cases, BB aerosols
179 have been reported to have reached as far as the adjacent Arctic region (Warneke et al., 2010; Generoso et al.,
180 2007). Van der Werf et al. (2006) estimated the emissions of BB aerosols from Eurasia to be much larger than
181 those from North America. Thus, it is not surprised that the concentrations of LEVO over the NWPO were much
182 higher than those over the eastern North Pacific and western North Atlantic at similar latitudes (Hu et al.,
183 2013b).

184 In addition, both galactosan and mannosan showed strong linear correlations with LEVO ($R^2 = 0.98$, $p < 0.05$)
185 in TSP collected over the NWPO and YBS in this study. These strong correlations indicate that the three tracers
186 were probably derived from the same BB sources. Previous studies have reported LEVO/mannosan (L/M) ratios
187 of 3–10, 15–25, and 25–40 from softwood, hardwood, and crop-residue burning, respectively (Kang et al., 2018;
188 Zhu et al., 2015). The calculated L/M ratios in TSP collected over the NWPO were 19 ± 4 in this study, which
189 implies dominant contributions from herbaceous plants and hardwood. The calculated L/M ratios in TSP
190 collected over the YBS were 14 ± 11 , indicating mixed sources.

191 In all, 5 of 13 samples collected over the SCS were classified into Category 1, with air masses identified as
192 originating from either the continental areas of South China or the Philippines (Fig. 2). The concentration of
193 LEVO fluctuated around $17 \pm 12 \text{ ng/m}^3$ in Category 1 but decreased to $3.6 \pm 3.4 \text{ ng/m}^3$ in Category 2. However, no
194 significant differences were found between categories due to the large variation in LEVO concentration among
195 the limited samples in Category 1 ($p > 0.05$). Forest fires occur accidentally, leading to the large variation in
196 LEVO in Category 1. Southern Asia has been reported to be one of the greatest emissions sources of BB
197 aerosols worldwide (van der Werf et al., 2006), which likely led to the higher mean value of LEVO in Category
198 1. However, the LEVO level observed over the SCS in Category 2 was closer to that reported from low-latitude
199 regions ($2.7 \pm 1.1 \text{ ng/m}^3$, Table 1) collected during a global circumnavigation cruise (Hu et al., 2013b). Hu et al.
200 (2013b) argued that their low observed concentrations may have been associated with intense wet deposition,
201 degradation as well as intensive moist convection that occurred in the tropical region during their summer cruise.
202 Unfortunately, no previous observations of LEVO in spring can allow us analyzing the long-term variation in
203 contribution of BB aerosols therein. However, this observation can be used for future comparison.



204

205

206

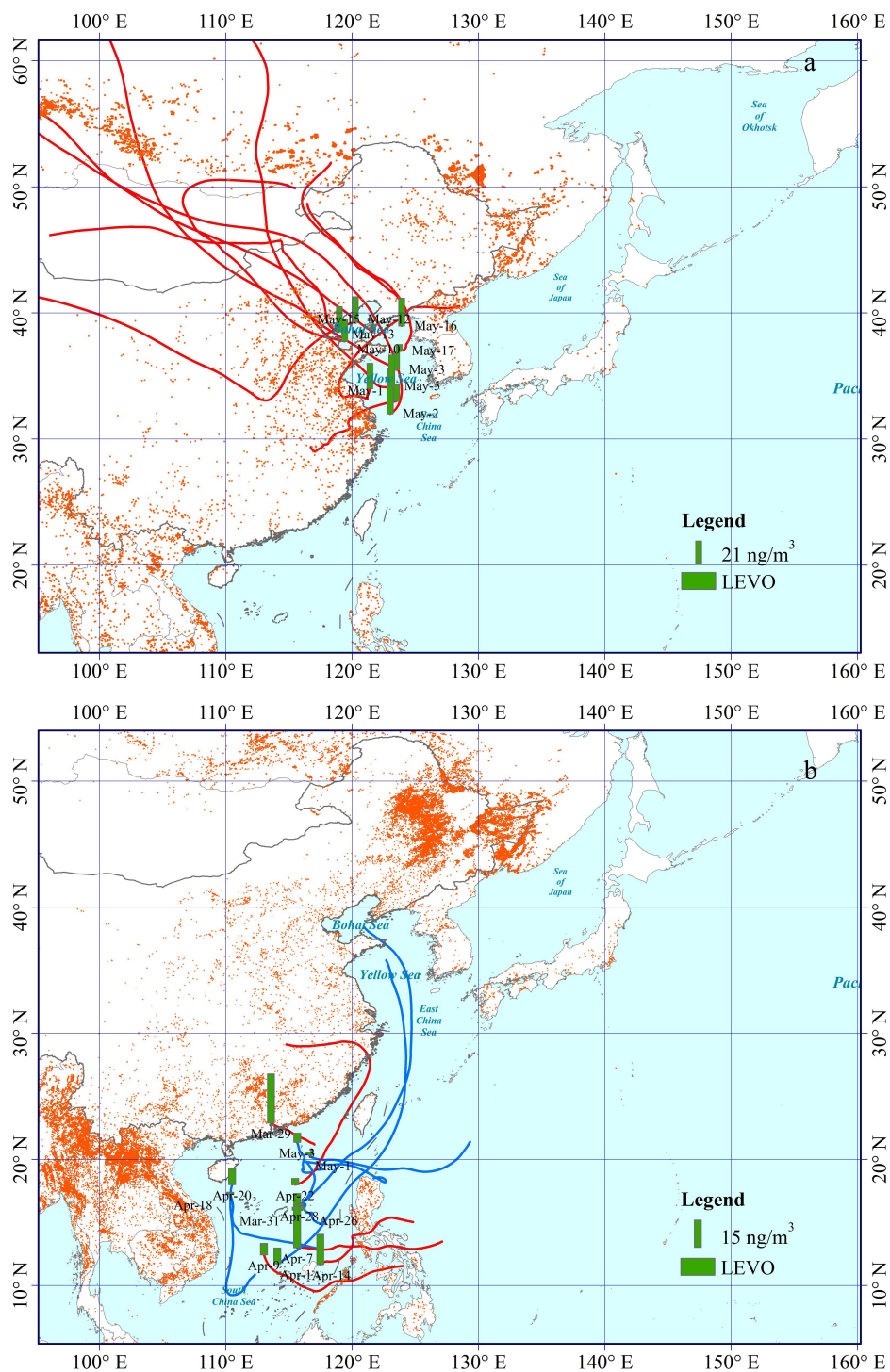
207

208

Figure 1. Spatial distribution of LEVO over the NWPO (2014) and BTs corresponding to the samples; the samples with the backward trajectories (red lines) indicate land-influenced aerosols (a, Category 1) and the blue line denotes ocean-influenced aerosols collected (b, Category 2). The red dots represent the locations of fires from Fire Information for Resource Management System (FIRMS,



209 <https://firms.modaps.eosdis.nasa.gov/>). The base map was from Resource and Environment Data Cloud
210 Platform, DOI: 10.12078/2018110201.



211
212 **Figure 2. Spatial distribution of LEVO over the YBS (a, 2014), and NWPO (b, 2017), detailed information**
213 **described in Figure 1.**

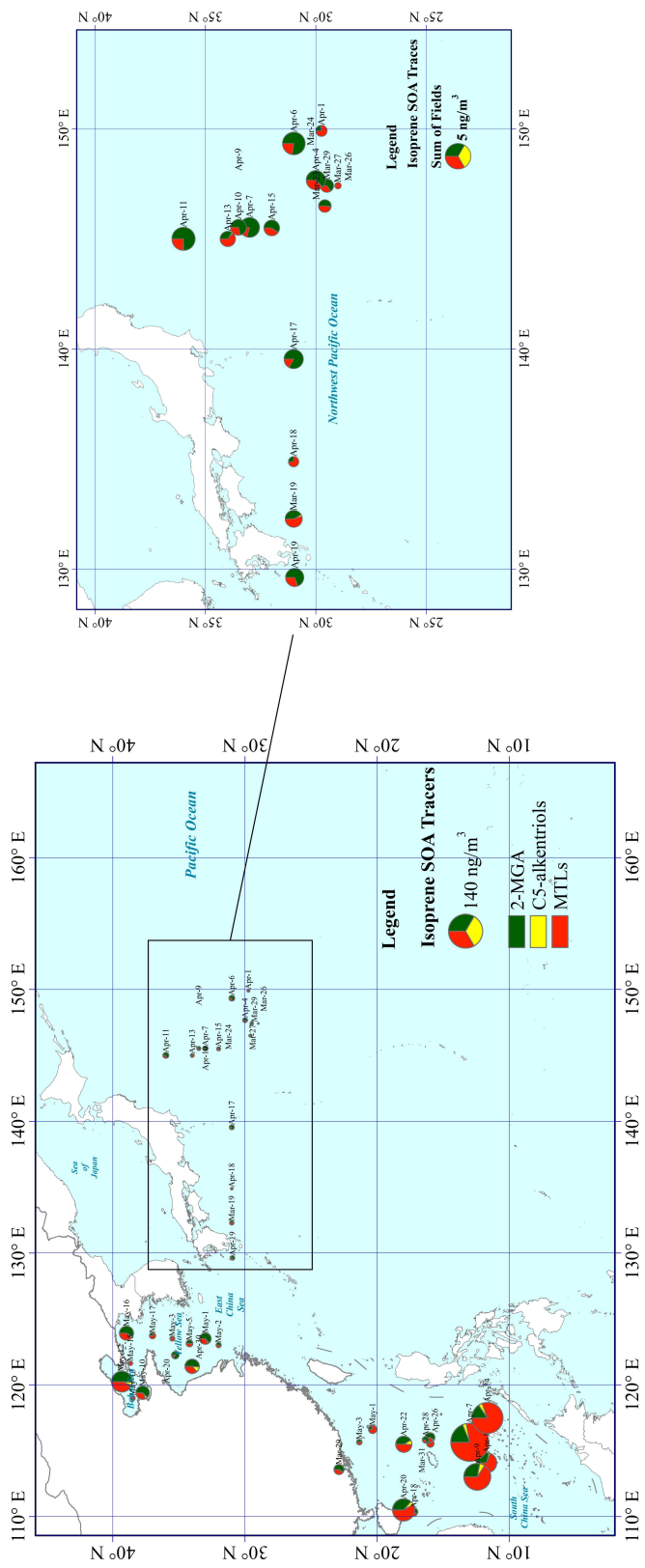


214

215 3.2 Spatiotemporal distributions of SOA₁ tracers

216 SOA₁ tracers were detected during all three cruises. The sum of SOA₁ tracers showed a decreasing trend of up to
217 approximately one order of magnitude from marginal seas to the open ocean, i.e., $45 \pm 54 \text{ ng/m}^3$ in TSP over the
218 SCS, $15 \pm 16 \text{ ng/m}^3$ over the YBS and $2.3 \pm 1.6 \text{ ng/m}^3$ over the NWPO (Fig. S1). The highest sum value of SOA₁
219 tracers over the SCS was 176 ng/m^3 , indicating strong photochemical formation of SOA from biogenic volatile
220 organics (Fig. 3). The geographical distribution of SOA₁ tracers in this study was generally consistent with those
221 reported by Hu et al. (2013a), with higher concentrations of these tracers in atmospheric particles collected from
222 low-latitude oceanic zones ($30^\circ \text{ S} - 30^\circ \text{ N}$) due to large emissions from tropical forests and strong photochemical
223 reactions. Their reported average contents of SOA₁ tracers in low-latitude oceanic zones fluctuated around
224 $9.2 \pm 6.7 \text{ ng/m}^3$, much lower than those measured in this study.

225 When the sum of SOA₁ tracers in each sample was examined separately according to the air mass source, a
226 significant difference was found over the SCS between Category 1 ($85 \pm 66 \text{ ng/m}^3$) and Category 2 (19 ± 22
227 ng/m^3), with significance at $p < 0.01$. The tracer values were $2.7 \pm 1.8 \text{ ng/m}^3$ in Category 1 and $1.7 \pm 1.0 \text{ ng/m}^3$ in
228 Category 2 over the NWPO, where no significant difference between the two categories was found ($p > 0.05$).
229 Supposed that concentrations of the tracers in Category 2 were completely contributed by marine sources, it can
230 be inferred that SOA₁ carried by continental air masses increased sharply over the SCS. However, it was not the
231 case over the NWPO. Because all samples over the YBS fell into Category 1, this comparison could not be
232 made for the YBS.



233
 234 **Figure 3.** Spatial distribution of SOA_i tracer compounds over three marine regions, ECS and NWPO in 2014, SCS in 2017. The area of the pie indicates the concentration of total
 235 SOA_i tracers. The base map was from Resource and Environment Data Cloud Platform, DOI: 10.12078/2018110201.



236 3.3 Spatiotemporal distributions of SOA_M, SOA_s tracers

237 The sum of SOA_M tracers including HGA, HD-MGA, and MBTCA was greatest over the SCS region (3.5±6.0
238 ng/m³), where the concentration was approximately double that over the YBS (1.6±2.0 ng/m³) and NWPO
239 regions (1.6±2.7 ng/m³) (Fig. S1), but no significant differences were identified between any two campaigns.
240 The concentrations of SOA_M tracers were almost one magnitude lower than those of SOA_I tracers. Due to the
241 unique contribution of terpene-derived SOA to nucleation and growth of newly formed particles in the
242 atmospheres (Gordon et al., 2017; Zhu et al., 2019; Ehn et al., 2014), the SOA_M may primarily cause indirect
243 climate effects rather than direct effects of aerosols in the marine atmosphere. The difference in mean SOA_M
244 concentration between the SCS and NWPO narrowed to a factor of two, in contrast to the differences of
245 approximately one order of magnitude in mean SOA_I between the two types of atmospheres. The precursors of
246 SOA_M tracers derive mainly from coniferous forests (Duhl et al., 2008) and the decreasing proportion of
247 coniferous forests in subtropical and tropical regions may partially explain the smaller spatial difference in
248 SOA_M tracers over the SCS compared to the YBS and NWPO. However, the comparable SOA_M levels over the
249 YBS and NWPO have not yet been explained.

250 Only three SOA_M tracers were measured in this study, but other SOA_M tracers have been measured and reported
251 in marine atmospheres (Kang et al., 2018; Fu et al., 2011). In order to compare our results with the total amount
252 of SOA_M tracers in the literature, the total amounts measured in this study were multiplied by a factor of 3.1
253 (described in supporting information Sect. S1, Fig. S4) according to the chamber results obtained by Kleindienst
254 et al. (2007). The adjusted values over the SCS were closer to the mean of 11.6 ng/m³ observed over the ECS
255 (Kang et al., 2018) and the lower values of 9.80–49.0 ng/m³ observed among 12 continental sites in China (Ding
256 et al., 2016). The adjusted total amounts of SOA_M over the NWPO and YBS were comparable to previous
257 observations of 3.0±5.0 ng/m³ collected from the Arctic to Antarctic in 2008–2010 (Hu et al., 2013a), but much
258 higher than observations of 63±49 pg/m³ over the North Pacific and Arctic in 2003 (Ding et al., 2013). This may
259 also imply a substantial increase in SOA_M in the last decades, although more investigations are needed to
260 confirm.

261 β-Caryophyllene is a major sesquiterpene emitted from plants such as Scots pine and European birch (Duhl et al.,
262 2008; Tarvainen et al., 2005). β-Caryophyllinic acid is formed through the ozonolysis or photo-oxidation of
263 β-caryophyllene. The highest levels of β-caryophyllinic acid were observed over the YBS (0.13±0.03 ng/m³),
264 followed by the SCS (0.08±0.11 ng/m³) and NWPO (0.05±0.09 ng/m³) (Fig. S1). The spatial distribution of
265 β-caryophyllinic acid clearly did not follow the general trend of biogenic SOA, with the highest values over the
266 SCS followed by the YBS. Compared to values from the literature, our results are much higher than those over
267 the North Pacific and Arctic Oceans (2.4±5.4 pg/m³) (Ding et al., 2013) but much lower than observations over
268 the East China Sea reported by Kang et al. (2018), where β-caryophyllinic acid was reported to be in the range
269 of 0.16–17.2 ng/m³ with a mean of 2.9 ng/m³. The large differences in β-caryophyllinic acid content observed in
270 various campaigns remains unexplained.

271 3.4 Spatiotemporal distributions of SOA_A tracers

272 When the concentrations of DHOPA in TSP were examined, the highest concentrations occurred over the SCS
273 (1.8±1.7 ng/m³), followed by the YBS (1.1±1.4 ng/m³), and the lowest values were recorded in the NWPO
274 region (0.3±0.5 ng/m³) (Fig. S1). The extent of the DHOPA decrease from the SCS to the NWPO was
275 approximately three times less than that of SOA_I tracers but approximately three times larger than that of SOA_M



276 tracers. Ding et al. (2017) reported annual averages of DHOPA among various sites in China, which ranged from
277 1.2 to 8.8 ng/m³. The concentrations of DHOPA observed over the SCS and the YBS were similar to the lower
278 values observed in upwind continental atmospheres.
279 Formation of DHOPA depends on the molecular structures of aromatics, as well as concentrations of free
280 radicals and oxidants, etc. (Li et al., 2016; Henze et al., 2008). The mean value of DHOPA in Category 1
281 (0.43±0.65 ng/m³) was nearly twice that in Category 2 (0.20±0.31 ng/m³) over the NWPO ($p > 0.05$). With two
282 samples with high DHOPA (1.2, 2.1 ng/m³) in Category 1 to be excluded, the recalculated average DHOPA
283 decrease down to 0.17±0.21 ng/m³. The continent-derived DHOPA seemingly yielded a minor contribution to
284 the observed values over the NWPO, except during strong long-range transport episodes. Similarly, the mean
285 values of DHOPA were same in Category 1 (1.8±2.1 ng/m³) and Category 2 (1.8±1.5 ng/m³) samples collected
286 over the SCS and no significant differences were observed between two categories. Much stronger UV radiation
287 occurs over the SCS than the YBS, which may contribute to the elevated DHOPA level over the SCS. Aside
288 from continent-derived precursors, oil exploration and heavy marine traffic over the SCS are also potential
289 contributors to the higher DHOPA levels therein, and this link requires further investigation. Previous field
290 observations in China have demonstrated that biofuel or biomass combustion emissions act as important sources
291 of aromatics in the atmosphere (Zhang et al., 2016), as evidenced by the association between the nationwide
292 increase in DHOPA during the cold period and the enhancement of BB emissions (Ding et al., 2017). In this
293 study, no linear correlation was obtained between DHOPA and LEVO in samples collected over the SCS and
294 other two campaigns, leaving emissions other than BB emissions as the major precursors for DHOPA in these
295 marine atmospheres (Li et al., 2013).

296 3.5 Causes for high photochemical yields of SOA_I over the SCS

297 Because higher concentrations of SOA_I were observed in TSP samples collected over the SCS, the composition
298 of SOA_I tracers was further investigated in terms of their formation pathways and sources. Based on the results
299 of chamber experiments, Surratt et al. (2010) proposed different formation mechanisms for 2-MGA and MTLs.
300 2-MGA is a C4-dihydroxycarboxylic acid, which forms through a high-NO_x pathway. MTLs and C5-alkene
301 triols are mainly products of the photooxidation of epoxydiols of isoprene under low-NO_x conditions.
302 MTLs acted as the dominant compounds among SOA_I tracers in most TSP samples collected over the SCS, with
303 concentrations of 31±42 ng/m³ (Fig. 3). The ratio of 2-MGA/MTLs ranged from 0.2 to 3.1, with a median value
304 of 0.6. The ratio exceeded the unity in only 4 of 13 samples. This result allowed us to infer that the observed
305 SOA_I tracers were generated mainly under low-NO_x conditions. Although the concentration of
306 2-methylerythritol was nearly double that of 2-methylthreitol, they were highly correlated ($R^2 = 0.99$, $p < 0.05$)
307 because of their shared formation pathway. Satellite data showed that the NO₂ levels in South China and the
308 Philippines were low, except in a few hotspots (Fig. S2). Such low-NO_x conditions favor the formation of
309 MTLs rather than 2-MGA over the tropical SCS. The isoprene emitted from plants growing on oceanic islands
310 may also undergo chemical conversion to SOA under low-NO_x conditions, and low-NO_x conditions are always
311 expected in remote marine atmospheres (Davis et al., 2001).
312 In general, zonally and monthly averaged OH concentrations around 15°N are ~50% greater than those around
313 35 °N (Bahm and Khalil, 2004). Thus, enhanced formation of MTLs is theoretically expected under the strong
314 UV radiation of tropical regions. However, no significant correlation between the concentrations of MTLs and
315 UV radiation was obtained over the SCS (data not shown) possibly due to the influences of various air masses.
316 A field study showed that MTL yields were positively correlated with ambient temperature in continental
317 atmospheres (Ding et al., 2011). 2-MGA yields, in contrast, showed no significant correlation with ambient



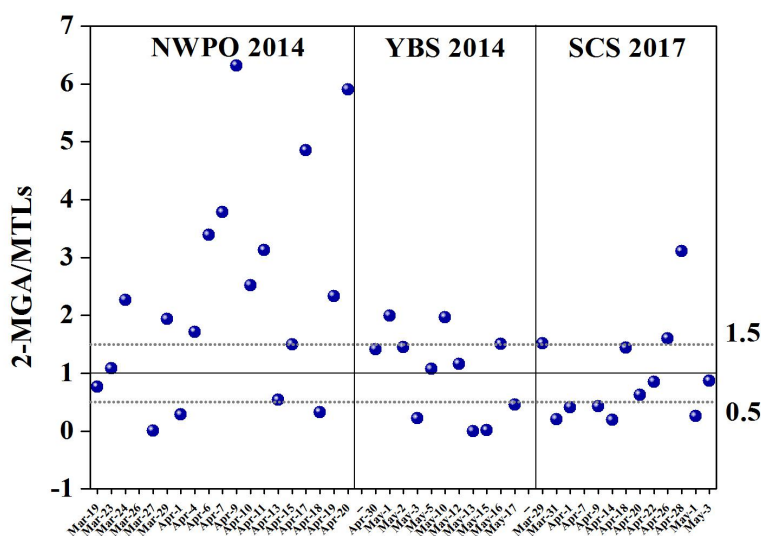
318 temperature in this study. Moreover, lower relative humidity may enhance the formation of 2-MGA in the
319 particulate phase but not for MTLs (Zhang et al., 2011). Variation in ambient temperature and relative humidity
320 may complicate the relationship between the concentrations of SOA_I tracers and UV radiation over the SCS.
321 In addition, the MTLs concentration in Category 1 (62 ± 55 ng/m³) was larger than that for Category 2 (11 ± 14
322 ng/m³). The more abundant MTLs associated with Category 1 was most likely related to long-range transport of
323 these chemicals from upwind continental areas, the oxidation of continental precursors in the marine atmosphere,
324 or both. Large emissions of isoprene were expected from tropical forests upwind of the SCS due to the high
325 vegetation coverage and high ambient temperature of such areas (Ding et al., 2011; Rinne et al., 2002). Global
326 estimates show tropical trees to be responsible for ~80% of terpenoid emissions and ~50% of other VOC
327 emissions (Guenther et al., 2012).
328 In a clean marine atmosphere, phytoplankton is the sole source of isoprene emissions over the oceans (Bonsang
329 et al., 1992; Broadgate et al., 1997). Chlorophyll-a has been widely employed as a measure of phytoplankton
330 abundance and a proxy for predicting isoprene concentrations in water (Hackenberg et al., 2017). The
331 satellite-derived chlorophyll-a level during the study period over the SCS was below 0.45 mg/m³, excluding
332 coastal areas (Fig. S3). The observations of 11 ± 14 ng/m³ in Category 2 should be considered as the upper
333 limitation value derived from marine phytoplankton in the SCS. Although air masses differed between
334 Categories 1 and 2, a good correlation was obtained between MTLs and 2-MGA when the data in the two
335 categories was pooled for analyses ($R^2 = 0.77$, $P < 0.01$). This strong correlation indicated these tracers are
336 primarily formed through shared pathways. However, this correlation was poor over the NWPO, as discussed
337 below.

338 3.6 Origin and formation of SOA_I over the NWPO

339 Over the NWPO, the concentration of 2-MGA was 1.6 ± 1.5 ng/m³, which was generally dominant among SOA_I
340 tracers, followed by MTLs (0.7 ± 0.3 ng/m³) and C5-alkene triols (0.03 ± 0.02 ng/m³). When the ratio of
341 2-MGA/MTLs was further examined, it varied greatly from <0.1 to 6.3, with a median value of 2.1. Most ratios
342 observed over the NWPO in this study were far greater than the values of 0.18–0.59 reported by Hu et al. (2013a)
343 from a global circumnavigation cruise, and also greater than 0.87–1.8 reported in urban areas of California
344 (Lewandowski et al., 2013) and the maximum value of 2.0 obtained over the YBS. Ding et al. (2013) also
345 reported ratios that fluctuated greatly from 0.5 to 10 with a median value of 3.3 during a summer cruise in the
346 NWPO and Arctic Ocean in 2003. The large 2-MGA/MTL ratios over the NWPO appeared to be highly
347 consistent over two independent sampling campaigns.
348 The compound profile of SOA_I tracers over the NWPO implied high-NO_x conditions allowing oxidation of
349 isoprene to generate the SOA_I present in most samples. Such high-NO_x conditions are impossible in a remote
350 marine atmosphere, as indicated in Figure S2. Regarding the lifespan of isoprene in the atmosphere is only
351 several hours (Bonsang et al., 1992), the long-range transport of oxidation products formed under high NO_x
352 levels over the continents likely led to the 2-MGA-dominated composition of SOA_I. Based on air mass back
353 trajectories, this long-range transport may involve 2-MGA originating from Siberia, northeastern China, or
354 Japan.
355 Organic aerosols over the NWPO were strongly influenced by forest fires that take place in Siberia during
356 spring and summer almost every year (Ding et al., 2013; Huang et al., 2009). Previous emissions inventory
357 studies have reported high isoprene and NO_x emissions from various BB types (Akagi et al., 2011; Andreae and
358 Merlet, 2001). Ding et al. (2013) thus argued that an increase in emissions of isoprene in the presence of BB,
359 followed by its chemical conversion under high-NO_x conditions, may lead to transport over thousands of



360 kilometers and hold at the detectable concentrations in the remote marine atmosphere over the NWPO. The
 361 same argument may hold true for the elevated ratios of 2-MGA/MTLs observed over the NWPO in this study
 362 (Fig. 4). However, we did not find a significant correlation between 2-MGA and LEVO over the NWPO.
 363 On the other hand, the ratios of 2-MGA/MTLs in 3 of 19 samples collected over the NWPO were below 0.5
 364 (Figure 4). In these cases, the oxidation of isoprene under low-NO_x conditions likely dominated the generation
 365 of SOA₁. The ratios of 2-MGA/MTLs were 0.5–1.5 in 4 of 19 samples, suggesting mixed contributions to SOA₁
 366 from the oxidation of isoprene under low-NO_x conditions and high-NO_x conditions. As the major formation
 367 pathways of 2-MGA and MTLs varied greatly among samples, no significant correlation ($R^2 = 0.12$, $p > 0.05$)
 368 was obtained between 2-MGA and MTLs over the NWPO. Recall that the tracer values of SOA₁ were 2.7 ± 1.8
 369 ng/m^3 in Category 1 and $1.7 \pm 1.0 \text{ ng/m}^3$ in Category 2. This implied that SOA₁ derived from marine sources was
 370 comparable to that derived from the continent outflows.



371
 372 **Figure 4. Spatial ratio of 2-MGA/MTLs among SOA₁ tracers over three marine regions.**

373 3.7 Source apportionment of secondary organic carbon (SOC)

374 The tracer-based approach developed by Kleindienst et al. (2007) was applied to estimate the concentrations of
 375 SOC and WSOC_{BB}, as follows:

$$[SOC] = \frac{\sum_i [tri]}{f_{SOC}} \quad (1)$$

$$[WSOC_{BB}] = \frac{C_{tracer}}{f_{tracer/WSOC_{BB}}} \quad (2)$$

378 where $\sum_i(tri)$ is the sum of concentrations of the selected suite of tracers for a precursor, and f_{SOC} is the mass
 379 fraction of tracer compounds in SOC generated from the precursor in chamber experiments. Assuming that the
 380 f_{SOC} values in ambient air match those in the chamber, the f_{SOC} values for precursors such as isoprene,
 381 monoterpenes, β -caryophyllene, and aromatics were $0.155 \pm 0.039 \mu\text{g}/\mu\text{gC}$, $0.231 \pm 0.111 \mu\text{g}/\mu\text{gC}$, 0.023 ± 0.0046



382 $\mu\text{g}/\mu\text{gC}$, and $0.00797 \pm 0.0026 \mu\text{g}/\mu\text{gC}$, respectively (Kleindienst et al., 2007), with uncertainty described in
383 Sect. S2. The fraction of LEVO in WSOC ($0.0994 \mu\text{g}/\mu\text{gC}$) from the BB plume was used for WSOC_{BB} (Ding et
384 al., 2008). The f_{SOC} value for monoterpenes was scaled up by a factor of 3.1 based on experimental observations,
385 as these two tracers (HGA+HD-MGA) accounted for 2/9 of the total tracers of monoterpenes, as described in
386 the supporting information (Kleindienst et al., 2007).

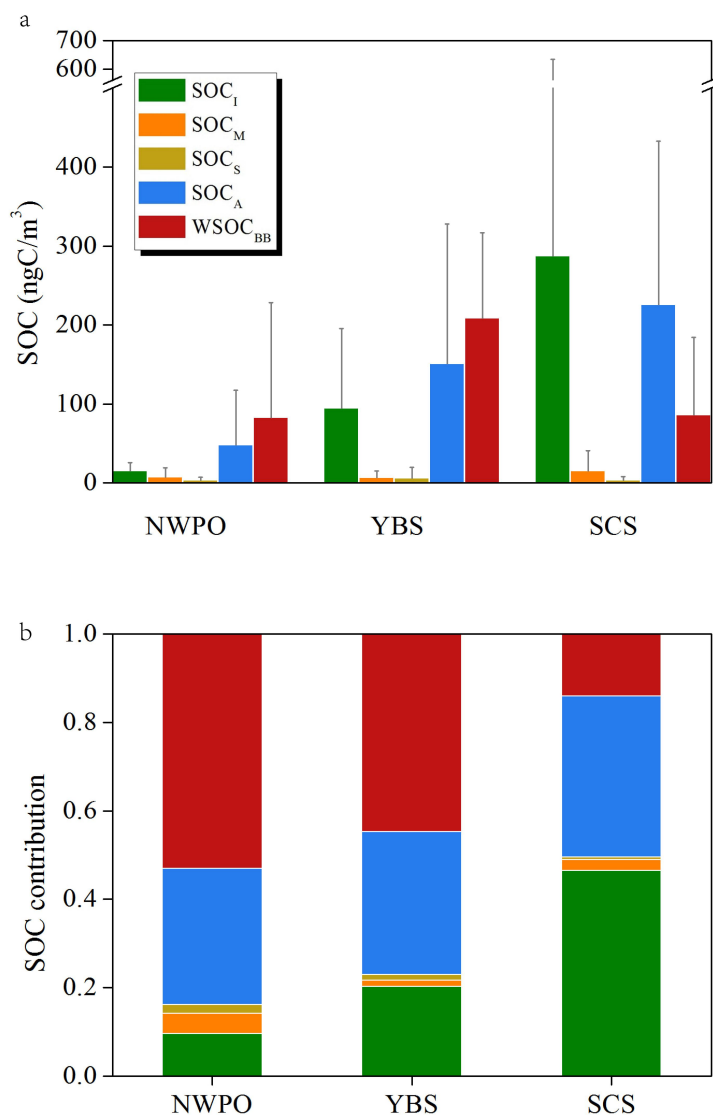
387 Over the SCS, nearly half of the sum of SOC and WSOC_{BB} was in the form of SOC_I (47%), followed by SOC_A
388 (36%), WSOC_{BB} (14%) and a minor contribution of 2.5% from SOC_M (Fig. 5). This composition pattern over
389 the SCS could be attributed to abundant biogenic SOA formation in low-latitude tropical marine atmospheres.
390 Over tropical marine regions, atmospheric oxidation products can account for 47–59% of the total organic
391 content estimated, with biomass burning emissions making up only 2–7% based on source apportionment using
392 organic tracers (Fu et al., 2011). A model study by Fu et al. (2012) showed that secondary formation accounts
393 for as much as 62% of OC estimated using tracers in eastern China in summer. A reverse pattern was observed
394 over the YBS, with WSOC_{BB} as the dominant contributor (45%) to the sum of SOC and WSOC_{BB}, followed by
395 SOC_A (32%) and SOC_I (20%). The contribution of SOC_M was also minor, at 1.5%. Notably, the chemical
396 composition observed over the NWPO was similar to that over the YBS, with WSOC_{BB} contributing up to 53%.
397 In addition, Kang et al. (2018) used the PMF method to identify various sources of OC in marine aerosols over
398 the ECS such as secondary nitrate, BSOA, BB, and fungal spores.

399 Geographically, the estimated SOC values from BVOCs ranked at the highest level of $306 \pm 343 \text{ ngC}/\text{m}^3$ over the
400 SCS, decreasing to $107 \pm 99 \text{ ngC}/\text{m}^3$ over the YBS and $24 \pm 22 \text{ ngC}/\text{m}^3$ over the NWPO. The estimates of
401 aromatic SOC exhibited the same geographic trend, with values of $225 \pm 208 \text{ ngC}/\text{m}^3$ over the SCS, 151 ± 177
402 ngC/m^3 over the YBS and $48 \pm 69 \text{ ngC}/\text{m}^3$ over the NWPO. Recent modeling results have also shown that
403 aromatic emissions are the predominant precursors of SOA during springtime in China in comparison with
404 BVOCs and other AVOCs (Han et al., 2016). Among estimates of WSOC_{BB}, the highest values of 209 ± 108
405 ngC/m^3 were recorded over the YBS, followed by comparable levels of $86 \pm 98 \text{ ngC}/\text{m}^3$ (SCS) and 83 ± 145
406 ngC/m^3 (NWPO).

407 In our study, the calculated WSOC_{BB} estimate accounted for $4.1 \pm 5.0\%$ and $3.3 \pm 1.7\%$ of measured OC over the
408 NWPO and YBS, respectively, and these values are higher than that obtained over the ECS during summer
409 (1.4%) (Kang et al., 2018). Estimated SOC from BVOCs accounted for only $1.5 \pm 1.4\%$ and $1.8 \pm 1.7\%$ to the
410 measured OC over the NWPO and YBS, respectively, which is lower than that over ECS (4.21%) (Kang et al.,
411 2018). However, the mean values obtained in this study were similar to the total SOC level estimated using
412 tracers as a proportion of measured WSOC (4%) during a cruise on the North Pacific and Arctic Oceans,
413 supposed that WSOC accounted for half of the total OC in atmospheric particles (Ding et al., 2013).

414 The calculated SOC level derived from organic tracers accounted for less than 6% of total measured OC in these
415 study areas. However, this SOC compounds are expected to derive mainly from photochemical reactions in the
416 gas phase, followed by gas-aerosol partitioning. These compounds likely play an important role in the growth of
417 newly formed particles alongside pre-existing nucleation mode or Aitken mode particles. However, most organic
418 matter detected in bulk samples may originate from primary sources, heterogenous reactions and in-cloud
419 processing (Ervens et al., 2011; Kanakidou et al., 2005; Nichols, 2016), and these compounds may be major
420 drivers of the direct climate effects of aerosols, rather than indirect climate effects. In the future, a
421 comprehensive combination measurement of organic tracers and organic matter with an aerosol mass
422 spectrometer should be used to elucidate the formation and growth processes of atmospheric nanoparticles.

423



424
425 **Figure 5. Average SOC levels calculated using the tracer-SOC/WSOC method over three marine regions**
426 **(ECS and NWPO in 2014, SCS in 2017) and their contributions based on five organic tracers measured in**
427 **this study.**

428 4. Conclusions

429 This study investigated the geographical distributions of tracer-based organic matter observations in TSP
430 collected over two marginal seas of China and the NWPO in the spring season, when the East Asian monsoon
431 carries biogenic and anthropogenic aerosols over these oceanic zones. We found that a significantly large
432 difference in LEVO over the NWPO between two categories of air masses originating from upwind continents
433 or oceanic regions, as Category 1 (continental) contained 13 ± 18 ng/m³ and Category 2 (oceanic) had 2.0 ± 1.8



434 ng/m³; the concentrations of LEVO in Category 2 were closer to the low values reported in the literature. This
435 further implied a large increase in contribution of continent-derived BB aerosols to marine atmospheres over the
436 NWPO in recent decades, compared to previous studies. Combining the L/M ratios of 19±4 over the NWPO
437 with the calculated air mass back trajectories indicates that the increase was very likely associated with
438 enhanced emissions of BB aerosols from wildfires in Siberia and northeastern China. Moreover, the mean level
439 of BB aerosols over the SCS nearly matched that over the NWPO. The contents of LEVO in Category 2 air
440 masses, derived from oceanic zones over the SCS, were comparable with those reported in the literature, but the
441 mean value was only about a quarter of that in Category 1, representing air masses from upwind continents.
442 However, the limited data available over the SCS in the literature cannot support inferences about whether BB
443 aerosols emitted from upwind tropical forests have increased in recent decades.

444 The concentrations of SOA_I over the SCS were approximately one order of magnitude greater than those
445 observed over the NWPO and several times larger than those over the YBS. The larger values observed over the
446 SCS in Category 1 than in Category 2 were likely driven by high emissions of isoprene from upwind tropical
447 forests and strong solar radiation. The MTLs dominance of SOA_I over the SCS strongly suggested that SOC
448 from BVOCs was generated primarily under low-NO_x conditions. On the other hand, 2-MGA dominance over
449 the YBS implied that most SOC was generated under high-NO_x conditions. Elevated ratios of 2-MGA/MTLs
450 of >1.5 were obtained for 11 of 19 total samples collected over the NWPO, consistent with those reported in the
451 literature. Larger ratios may be attributed to possible emissions of BVOCs in the presence of BB. However, the
452 comparable concentrations of SOA_I in Category 1 and Category 2 samples collected over the NWPO implied a
453 large contribution of SOA_I from marine sources. The aromatic SOA tracers' levels were highest over the SCS,
454 followed by values obtained over the YBS and NWPO. The high values observed over the SCS may be related
455 to strong solar radiation, but the sources of precursors remain unexplained. Based on the concentrations in
456 Category 1 and 2 air samples collected over the SCS and NWPO, mixed sources of aromatic VOCs should exist,
457 including continent-derived precursors, oil exploration and heavy marine traffic.

458 Over the NWPO and the YBS, the estimated WSOC_{BB} levels were nearly equal to the sum of SOC estimated
459 from the oxidation of aromatics and BVOCs. Over the SCS, SOC estimated from the oxidation of BVOCs was
460 significantly larger than the estimated WSOC_{BB}. The geographical difference may be related to emissions of
461 primary particulate organics and gaseous precursors as well as formation processing of secondary organics in
462 various atmospheres.

463 The atmospheric composition of SOA in different geographical locations is, however, highly complex and is
464 regulated by many factors including local meteorological conditions, anthropogenic emissions, plant species,
465 vegetation cover and regional chemistry, and therefore warrants further quantification and analyses. Particularly,
466 whether BB aerosols and other biogenic organic aerosols in marine atmospheres will continuously increase
467 under warming conditions.



468 Table 1. Sum of organic tracer contents (ng/m³) at different locations worldwide.

Site	Date	Sampler	LEVO	SOA _I	SOA _M	SOA _S	SOA _A	Reference
Wakayama, Japan (Forest)	August 20–30, 2010, Day	TSP	2.5±2.1	281±274	54.6±50.2	1.2±1.2		(Zhu et al., 2016a)
	Night		1.1±0.9	199±207	36.3±33.6	0.9±0.8		
Across China	summer 2012	Anderson sampler		123±79	10.5±6.6	5.0±4.0	2.9±1.5	(Ding et al., 2014)
Beijing (PKU) (urban site)	summer 2007	PM2.5	37-148	59±32	30±14	2.7±1.0		(Yang et al., 2016)
Beijing (YUFA) (suburban site)			34-149	75±43	32±14	3.9±1.5		
Shanghai (BS) (Suburban site)	Apr-May 2010	PM2.5	88.8±57.2	3.8±3.9	6.1±3.7	1.0±0.7	1.1±0.7	(Feng et al., 2013)
Shanghai (XJH) (Urban site)			58.3±27.5	2.5±1.7	2.7±1.3	0.4±0.3	0.6±0.4	
Mt. Tai	summer 2014	PM2.5		56.4±45.6	34.4±28.4			(Zhu et al., 2017)
Central Pearl River Delta	fall-winter 2007	PM2.5		30.8±15.9	6.6±4.4	0.5±0.6		(Ding et al., 2011)
Central Tibetan Plateau	2012-2013	Anderson sampler		26.6±44.2	1.0±0.6	0.09±0.1	0.3±0.2	(Shen et al., 2015)
Mumbai, India	winter 2007	PM10		4.1±2.4	29±22		0.6±0.6	(Fu et al., 2016)
	summer 2007			1.1±0.7	9.4±4.7		0.05±0.1	
Alaska	Spring 2009	TSP		2.4	3.6	0.9		(Haque et al., 2016)
	2008-2009	TSP		4.1	2.0	1.5		
SYS	Spring 2017	TSP	9.6±8.6	45±54	3.5±6.0	0.07±0.1	1.8±1.7	This study
YBS	Spring 2014	TSP	21±11	15±16	1.6±2.0	0.1±0.3	1.1±1.4	This study
NWPO	Spring 2014	TSP	8.2±14	2.3±1.6	1.6±2.7	0.05±0.09	0.3±0.5	This study
East China Sea	18 May to 12 June 2014	TSP	0.09–64.3 (7.3)	0.15–64.0 (8.4)	0.26–87.2 (11.6)	0.16–17.2 (2.9)		(Kang et al., 2018)
Arctic to Antarctic	July to September 2008; November 2009 to April 2010	TSP	5.4±6.2	8.5±11	3.0±5.0			(Hu et al., 2013a; Hu et al., 2013b)
North Pacific	2003	TSP		0.5±0.4	0.6±0.4	0.06±0.05	0.002±0.005	(Ding et al., 2013)





470 **Data availability.** Most of the data are shown in supplement. Other data are available by contacting the
471 corresponding author.

472 **Supplement.** The supplement related to this article is available.

473 **Author contributions.** XY, TG and JF conceived and led the studies. TG, JW and JF carried out the
474 experiments and analyzed the data. TG and JF interpreted the results. ZG, JF, HG discussed the results and
475 commented on the manuscript. TG prepared the manuscript with contributions from all the co-authors.

476 **Competing interests.** The authors declare that they have no conflict of interest.

477 **Acknowledgements.** This research has been supported by the National Key Research and Development
478 Program in China (No.2016YFC0200504) and the Natural Science Foundation of China (Grant No. 41776086).

479

480 **References:**

- 481 Ait-Helal, W., Borbon, A., Sauvage, S., de Gouw, J. A., Colomb, A., Gros, V., Freutel, F., Crippa, M., Afif, C.,
482 Baltensperger, U., Beekmann, M., Doussin, J.-F., Durand-Jolibois, R., Fronval, I., Grand, N., Leonardis, T.,
483 Lopez, M., Michoud, V., Miet, K., Perrier, S., Prévôt, A. S. H., Schneider, J., Siour, G., Zapf, P., and Locoge, N.:
484 Volatile and intermediate volatility organic compounds in suburban Paris: variability, origin and importance for
485 SOA formation, *Atmos. Chem. Phys.*, 14, 10439-10464, <https://doi.org/10.5194/acp-14-10439-2014>, 2014.
- 486 Akagi, S. K., Yokelson, R. J., Wiedinmyer, C., Alvarado, M. J., Reid, J. S., Karl, T., Crounse, J. D., and
487 Wennberg, P. O.: Emission factors for open and domestic biomass burning for use in atmospheric models,
488 *Atmos. Chem. Phys.*, 11, 4039-4072, <https://doi.org/10.5194/acp-11-4039-2011>, 2011.
- 489 Andreae, M. O. and Merlet, P.: Emission of trace gases and aerosols from biomass burning, *Global Biogeochem.*
490 *Cy.*, 15, 955-966, 2001.
- 491 Bahm, K. and Khalil, M. A. K.: A new model of tropospheric hydroxyl radical concentrations, *Chemosphere*, 54,
492 143-166, <https://doi.org/10.1016/j.chemosphere.2003.08.006>, 2004.
- 493 Bao, H., Niggemann, J., Luo, L., Dittmar, T., and Kao, S.: Molecular composition and origin of water-soluble
494 organic matter in marine aerosols in the Pacific off China, *Atmos. Environ.*, 191, 27-35,
495 <https://doi.org/10.1016/j.atmosenv.2018.07.059>, 2018.
- 496 Bonsang, B., Polle, C., and Lambert, G.: Evidence for marine production of isoprene, *Geophys. Res. Lett.*, 19,
497 1129-1132, 1992.
- 498 Bougiatioti, A., Bezantakos, S., Stavroulas, I., Kalivitis, N., Kokkalis, P., Biskos, G., Mihalopoulos, N.,
499 Papayannis, A., and Nenes, A.: Biomass-burning impact on CCN number, hygroscopicity and cloud formation
500 during summertime in the eastern Mediterranean, *Atmos. Chem. Phys.*, 16, 7389-7409,
501 <https://doi.org/10.5194/acp-16-7389-2016>, 2016.
- 502 Broadgate, W. J., Liss, P. S., and Penkett, S. A.: Seasonal emissions of isoprene and other reactive hydrocarbon
503 gases from the ocean, *Geophys. Res. Lett.*, 24, 2675-2678, 1997.
- 504 Chen, J., Li, C., Ristovski, Z., Milic, A., Gu, Y., Islam, M. S., Wang, S., Hao, J., Zhang, H., He, C., Guo, H., Fu,
505 H., Miljevic, B., Morawska, L., Thai, P., LAM, Y. F., Pereira, G., Ding, A., Huang, X., and Dumka, U. C.: A
506 review of biomass burning: Emissions and impacts on air quality, health and climate in China, *Sci. Total*
507 *Environ.*, 579, 1000-1034, <https://doi.org/10.1016/j.scitotenv.2016.11.025>, 2017.



- 508 Claeys, M., Graham, B., Vas, G., Wang, W., Vermeylen, R., Pashynska, V., Cafmeyer, J., Guyon, P., Andreae,
509 M. O., Artaxo, P., and Maenhaut, W.: Formation of secondary organic aerosols through photooxidation of
510 isoprene, *Science*, 303, 1173-1176, 2004.
- 511 Davis, D. D., Grodzinsky, G., Kasibhatla, P., Crawford, J., Chen, G., Liu, S., Bandy, A., Thornton, D., Guan, H.,
512 and Sandholm, S.: Impact of ship emissions on marine boundary layer NO_x and SO₂ distributions over the
513 Pacific Basin, *Geophys. Res. Lett.*, 28, 235-238, 2001.
- 514 Ding, X., Zheng, M., Yu, L., Zhang, X., Weber, R. J., Yan, B., Russell, A. G., Edgerton, E. S., and Wang, X.:
515 Spatial and seasonal trends in biogenic secondary organic aerosol tracers and water-soluble organic carbon in
516 the southeastern United States, *Environ. Sci. Technol.*, 42, 5171-5176, <https://doi.org/10.1021/es7032636>, 2008.
- 517 Ding, X., Wang, X., and Zheng, M.: The influence of temperature and aerosol acidity on biogenic secondary
518 organic aerosol tracers: Observations at a rural site in the central Pearl River Delta region, South China, *Atmos.*
519 *Environ.*, 45, 1303-1311, <https://doi.org/10.1016/j.atmosenv.2010.11.057>, 2011.
- 520 Ding, X., Wang, X., Xie, Z., Zhang, Z., and Sun, L.: Impacts of Siberian biomass burning on organic aerosols
521 over the North Pacific Ocean and the Arctic: Primary and secondary organic tracers, *Environ. Sci. Technol.*, 47,
522 3149-3157, <https://doi.org/10.1021/es3037093>, 2013.
- 523 Ding, X., He, Q., Shen, R., Yu, Q., and Wang, X.: Spatial distributions of secondary organic aerosols from
524 isoprene, monoterpenes, β -caryophyllene, and aromatics over China during summer, *J. Geophys. Res.-Atmos.*,
525 119, 877-891, <https://doi.org/10.1002/2014JD021748>, 2014.
- 526 Ding, X., Zhang, Y., He, Q., Yu, Q., Shen, R., Zhang, Y., Zhang, Z., Lyu, S., Hu, Q., Wang, Y., Li, L., Song,
527 W., and Wang, X.: Spatial and seasonal variations of secondary organic aerosol from terpenoids over China, *J.*
528 *Geophys. Res.-Atmos.*, 121, 661-678, <https://doi.org/10.1002/2016JD025467>, 2016.
- 529 Ding, X., Zhang, Y., He, Q., Yu, Q., Wang, J., Shen, R., Song, W., Wang, Y., and Wang, X.: Significant
530 increase of aromatics-derived secondary organic aerosol during fall to winter in China, *Environ. Sci. Technol.*,
531 51, 7432-7441, <https://doi.org/10.1021/acs.est.6b06408>, 2017.
- 532 Duhl, T. R., Helmig, D., and Guenther, A.: Sesquiterpene emissions from vegetation: a review, *Biogeosciences*,
533 5, 761-777, <https://doi.org/10.5194/bg-5-761-2008>, 2008,
- 534 Ehn, M., Thornton, J. A., Kleist, E., Sipilä, M., Junninen, H., Pullinen, I., Springer, M., Rubach, F., Tillmann, R.,
535 Lee, B., Lopez-Hilfiker, F., Andres, S., Acir, I.-H., Rissanen, M., Jokinen, T., Schobesberger, S., Kangasluoma,
536 J., Kontkanen, J., Nieminen, T., Kurtén, T., Nielsen, L. B., Jørgensen, S., Kjaergaard, H. G., Canagaratna, M.,
537 Dal Maso, M., Berndt, T., Petäjä, T., Wahner, A., Kerminen, V.-M., Kulmala, M., Worsnop, D. R., Wildt, J.,
538 and Mentel, T. F.: A large source of low volatility secondary organic aerosol, *Nature*, 506, 476-479,
539 <https://doi.org/10.1038/nature13032>, 2014.
- 540 Ekström, S., Nozière, B., and Hansson, H.: The Cloud Condensation Nuclei (CCN) properties of 2-methyltetrols
541 and C3-C6 polyols from osmolality and surface tension measurements, *Atmos. Chem. Phys.*, 9, 973-980, 2009.
- 542 Ervens, B., Turpin, B. J., and Weber, R. J.: Secondary organic aerosol formation in cloud droplets and aqueous
543 particles (aqSOA): a review of laboratory, field and model studies, *Atmos. Chem. Phys.*, 11, 11069-11102,
544 <https://doi.org/10.5194/acp-11-11069-2011>, 2011.
- 545 Feng, J. L., Guo, Z. G., Zhang, T. R., Yao, X. H., Chan, C. K., and Fang, M.: Source and formation of
546 secondary particulate matter in PM_{2.5} in Asian continental outflow, *J. Geophys. Res.-Atmos.*, 117, D03302,
547 <https://doi.org/10.1029/2011JD016400>, 2012.
- 548 Feng, J., Li, M., Zhang, P., Gong, S., Zhong, M., Wu, M., Zheng, M., Chen, C., Wang, H., and Lou, S.:
549 Investigation of the sources and seasonal variations of secondary organic aerosols in PM_{2.5} in Shanghai with
550 organic tracers, *Atmos. Environ.*, 79, 614-622, <https://doi.org/10.1016/j.atmosenv.2013.07.022>, 2013.
- 551 Fu, P., Kawamura, K., and Miura, K.: Molecular characterization of marine organic aerosols collected during a
552 round-the-world cruise, *J. Geophys. Res.-Atmos.*, 116, D13302, <https://doi.org/10.1029/2011JD015604>, 2011.
- 553 Fu, P., Aggarwal, S. G., Chen, J., Li, J., Sun, Y., Wang, Z., Chen, H., Liao, H., Ding, A., Umarji, G. S., Patil, R.
554 S., Chen, Q., and Kawamura, K.: Molecular markers of secondary organic aerosol in Mumbai, India, *Environ.*
555 *Sci. Technol.*, 50, 4659-4667, <https://doi.org/10.1021/acs.est.6b00372>, 2016.



- 556 Fu, T. M., Cao, J. J., Zhang, X. Y., Lee, S. C., Zhang, Q., Han, Y. M., Qu, W. J., Han, Z., Zhang, R., Wang, Y.
557 X., Chen, D., and Henze, D. K.: Carbonaceous aerosols in China: top-down constraints on primary sources and
558 estimation of secondary contribution, *Atmos. Chem. Phys.*, 12, 2725-2746,
559 <https://doi.org/10.5194/acp-12-2725-2012>, 2012.
- 560 Generoso, S., Bey, I., Attié, J., and Bréon, F.: A satellite- and model-based assessment of the 2003 Russian fires:
561 Impact on the Arctic region, *J. Geophys. Res.-Atmos.*, 112, D15302, <https://doi.org/10.1029/2006JD008344>,
562 2007.
- 563 Gordon, H., Kirkby, J., Baltensperger, U., Bianchi, F., Breitenlechner, M., Curtius, J., Dias, A., Dommen, J.,
564 Donahue, N. M., Dunne, E. M., Duplissy, J., Ehrhart, S., Flagan, R. C., Frege, C., Fuchs, C., Hansel, A., Hoyle,
565 C. R., Kulmala, M., Kürten, A., Lehtipalo, K., Makhmutov, V., Molteni, U., Rissanen, M. P., Stozhkov, Y.,
566 Tröstl, J., Tsagkogeorgas, G., Wagner, R., Williamson, C., Wimmer, D., Winkler, P. M., Yan, C., and Carslaw,
567 K. S.: Causes and importance of new particle formation in the present-day and preindustrial atmospheres, *J.*
568 *Geophys. Res.-Atmos.*, 122, 8739–8760, <https://doi.org/10.1002/2017JD026844>, 2017.
- 569 Guenther, A., Karl, T., Harley, P., Wiedinmyer, C., Palmer, P. I., and Geron, C.: Estimates of global terrestrial
570 isoprene emissions using MEGAN (Model of Emissions of Gases and Aerosols from Nature), *Atmos. Chem.*
571 *Phys.*, 6, 3181-3210, 2006.
- 572 Guenther, A. B., Jiang, X., Heald, C. L., Sakulyanontvittaya, T., Duhl, T., Emmons, L. K., and Wang, X.: The
573 Model of Emissions of Gases and Aerosols from Nature version 2.1 (MEGAN2.1): an extended and updated
574 framework for modeling biogenic emissions, *Geosci. Model Dev.*, 5, 1471-1492,
575 <https://doi.org/10.5194/gmd-5-1471-2012>, 2012.
- 576 Hackenberg, S. C., Andrews, S. J., Airs, R., Arnold, S. R., Bouman, H. A., Brewin, R. J. W., Chance, R. J.,
577 Cummings, D., Dall'Olmo, G., Lewis, A. C., Minaeian, J. K., Reifel, K. M., Small, A., Tarran, G. A., Tilstone,
578 G. H., and Carpenter, L. J.: Potential controls of isoprene in the surface ocean, *Global Biogeochem. Cy.*, 31,
579 644-662, <https://doi.org/10.1002/2016GB005531>, 2017.
- 580 Han, Z., Xie, Z., Wang, G., Zhang, R., and Tao, J.: Modeling organic aerosols over east China using a volatility
581 basis-set approach with aging mechanism in a regional air quality model, *Atmos. Environ.*, 124, 186-198,
582 <https://doi.org/10.1016/j.atmosenv.2015.05.045>, 2016.
- 583 Haque, M. M., Kawamura, K., and Kim, Y.: Seasonal variations of biogenic secondary organic aerosol tracers in
584 ambient aerosols from Alaska, *Atmos. Environ.*, 130, 95-104, 2016.
- 585 Heald, C. L., Henze, D. K., Horowitz, L. W., Feddesma, J., Lamarque, J.-F., Guenther, A., Hess, P. G., Vitt, F.,
586 Seinfeld, J. H., Goldstein, A. H., and Fung, I.: Predicted change in global secondary organic aerosol
587 concentrations in response to future climate, emissions, and land use change, *J. Geophys. Res.-Atmos.*, 113,
588 D05211, <https://doi.org/10.1029/2007JD009092>, 2008.
- 589 Henze, D. K., Seinfeld, J. H., Ng, N. L., Kroll, J. H., Fu, T.-M., Jacob, D. J., and Heald, C. L.: Global modeling
590 of secondary organic aerosol formation from aromatic hydrocarbons: high-vs. low-yield pathways, *Atmos.*
591 *Chem. Phys.*, 8, 2405-2420, 2008.
- 592 Hsiao, T., Ye, W., Wang, S., Tsay, S., Chen, W., Lin, N., Lee, C., Hung, H., Chuang, M., and Chantara, S.:
593 Investigation of the CCN activity, BC and UVBC mass concentrations of biomass burning aerosols during the
594 2013 BASELInE campaign, *Aerosol Air Qual. Res.*, 16, 2742-2756, <https://doi.org/10.4209/aaqr.2015.07.0447>,
595 2016.
- 596 Hu, D. and Yu, J. Z.: Secondary organic aerosol tracers and malic acid in Hong Kong: seasonal trends and
597 origins, *Environ. Chem.*, 10, 381–394, <https://doi.org/10.1071/EN13104>, 2013.
- 598 Hu, Q., Xie, Z., Wang, X., Kang, H., He, Q., and Zhang, P.: Secondary organic aerosols over oceans via
599 oxidation of isoprene and monoterpenes from Arctic to Antarctic, *Sci. Rep.-UK*, 3, 2280,
600 <https://doi.org/10.1038/srep02280>, 2013a.
- 601 Hu, Q., Xie, Z., Wang, X., Kang, H., and Zhang, P.: Levoglucosan indicates high levels of biomass burning
602 aerosols over oceans from the Arctic to Antarctic, *Sci. Rep.-UK*, 3, 3119, <https://doi.org/10.1038/srep03119>,
603 2013b.



- 604 Hu, Q., Qu, K., Gao, H., Cui, Z., Gao, Y., and Yao, X.: Large increases in primary trimethylaminium and
605 secondary dimethylaminium in atmospheric particles associated with cyclonic eddies in the Northwest Pacific
606 Ocean, *J. Geophys. Res.-Atmos.*, 123, 133-146, <https://doi.org/10.1029/2018JD028836>, 2018.
- 607 Huang, S., Siegert, F., Goldammer, J. G., and Sukhinin, A. I.: Satellite-derived 2003 wildfires in southern
608 Siberia and their potential influence on carbon sequestration, *Int. J. Remote Sens.*, 30, 1479-1492,
609 <https://doi.org/10.1080/01431160802541549>, 2009.
- 610 John, J. G., Stock, C. A., and Dunne, J. P.: A more productive, but different, ocean after mitigation, *Geophys.*
611 *Res. Lett.*, 42, 9836-9845, <https://doi.org/10.1002/2015GL066160>, 2015.
- 612 Kanakidou, M., Seinfeld, J. H., Pandis, S. N., Barnes, I., Dentener, F. J., Facchini, M. C., Van Dingenen, R.,
613 Ervens, B., Nenes, A., Nielsen, C. J., Swietlicki, E., Putaud, J. P., Balkanski, Y., Fuzzi, S., Horth, J., Moortgat,
614 G. K., Winterhalter, R., Myhre, C. E. L., Tsigaridis, K., Vignati, E., Stephanou, E. G., and Wilson, J.: Organic
615 aerosol and global climate modelling: a review, *Atmos. Chem. Phys.*, 5, 1053-1123,
616 <https://doi.org/10.5194/acp-5-1053-2005>, 2005.
- 617 Kang, M., Fu, P., Kawamura, K., Yang, F., Zhang, H., Zang, Z., Ren, H., Ren, L., Zhao, Y., Sun, Y., and Wang,
618 Z.: Characterization of biogenic primary and secondary organic aerosols in the marine atmosphere over the East
619 China Sea, *Atmos. Chem. Phys.*, 18, 13947-13967, <https://doi.org/10.5194/acp-18-13947-2018>, 2018.
- 620 Kang, M., Guo, H., Wang, P., Fu, P., Ying, Q., Liu, H., Zhao, Y., and Zhang, H.: Characterization and source
621 apportionment of marine aerosols over the East China Sea, *Sci. Total Environ.*, 651, 2679-2688,
622 <https://doi.org/10.1016/j.scitotenv.2018.10.174>, 2019.
- 623 Kawamura, K., Hoque, M. M. M., Bates, T. S., and Quinn, P. K.: Molecular distributions and isotopic
624 compositions of organic aerosols over the western North Atlantic: Dicarboxylic acids, related compounds,
625 sugars, and secondary organic aerosol tracers, *Org. Geochem.*, 113, 229-238,
626 <https://doi.org/10.1016/j.orggeochem.2017.08.007>, 2017.
- 627 Kleindienst, T. E., Jaoui, M., Lewandowski, M., Offenberg, J. H., Lewis, C. W., Bhave, P. V., and Edney, E. O.:
628 Estimates of the contributions of biogenic and anthropogenic hydrocarbons to secondary organic aerosol at a
629 southeastern US location, *Atmos. Environ.*, 41, 8288-8300, <https://doi.org/10.1016/j.atmosenv.2007.06.045>,
630 2007.
- 631 Lauvset, S. K., Tjiputra, J., and Muri, H.: Climate engineering and the ocean: effects on biogeochemistry and
632 primary production, *Biogeosciences*, 14, 5675-5691, <https://doi.org/10.5194/bg-14-5675-2017>, 2017.
- 633 Lewandowski, M., Piletic, I. R., Kleindienst, T. E., Offenberg, J. H., Beaver, M. R., Jaoui, M., Docherty, K. S.,
634 and Edney, E. O.: Secondary organic aerosol characterisation at field sites across the United States during the
635 spring-summer period, *Int. J. Environ. Anal. Chem.*, 93, 1084-1103,
636 <https://doi.org/10.1080/03067319.2013.803545>, 2013.
- 637 Li, L., Tang, P., Nakao, S., Kacarab, M., and Cocker, D. R.: Novel approach for evaluating secondary organic
638 aerosol from aromatic hydrocarbons: unified method for predicting aerosol composition and formation, *Environ.*
639 *Sci. Technol.*, 50, 6249-6256, <https://doi.org/10.1021/acs.est.5b05778>, 2016.
- 640 Li, M., Zhang, Q., Streets, D. G., He, K. B., Cheng, Y. F., Emmons, L. K., Huo, H., Kang, S. C., Lu, Z., Shao,
641 M., Su, H., Yu, X., and Zhang, Y.: Mapping Asian anthropogenic emissions of non-methane volatile organic
642 compounds to multiple chemical mechanisms, *Atmos. Chem. Phys.*, 14, 5617-5638, 2014.
- 643 Meskhidze, N. and Nenes, A.: Phytoplankton and cloudiness in the Southern Ocean, *Science*, 314, 1419-1423,
644 <https://doi.org/10.1126/science.1131779>, 2006.
- 645 Mochida, M., Kawamura, K., Fu, P., and Takemura, T.: Seasonal variation of levoglucosan in aerosols over the
646 western North Pacific and its assessment as a biomass-burning tracer, *Atmos. Environ.*, 44, 3511-3518,
647 <https://doi.org/10.1016/j.atmosenv.2010.06.017>, 2010.
- 648 Murphy, D. M., Chow, J. C., Leibensperger, E. M., Malm, W. C., Pitchford, M., Schichtel, B. A., Watson, J. G.,
649 and White, W. H.: Decreases in elemental carbon and fine particle mass in the United States, *Atmos. Chem.*
650 *Phys.*, 11, 4679-4686, <https://doi.org/10.5194/acp-11-4679-2011>, 2011.
- 651 Nichols, M. A.: Spatial and temporal variability of marine primary organic aerosols over the global oceans: a



- 652 review, University of Maryland College Park, 2016.
- 653 Peñuelas, J. and Staudt, M.: BVOCs and global change, *Trends Plant Sci.*, 15, 133-144,
654 <https://doi.org/10.1016/j.tplants.2009.12.005>, 2010.
- 655 Rinne, H. J. I., Guenther, A. B., Greenberg, J. P., and Harley, P. C.: Isoprene and monoterpene fluxes measured
656 above Amazonian rainforest and their dependence on light and temperature, *Atmos. Environ.*, 36, 2421-2426,
657 [https://doi.org/10.1016/S1352-2310\(01\)00523-4](https://doi.org/10.1016/S1352-2310(01)00523-4), 2002.
- 658 Running, S. W.: Is global warming causing more, larger wildfires? *Science*, 313, 927-928,
659 <https://doi.org/10.1126/science.1130370>, 2006.
- 660 Sharma, S., Lavoué, D., Cachier, H., Barrie, L. A., and Gong, S. L.: Long-term trends of the black carbon
661 concentrations in the Canadian Arctic, *J. Geophys. Res.-Atmos.*, 109, D15203,
662 <https://doi.org/10.1029/2003JD004331>, 2004.
- 663 Shen, R., Ding, X., He, Q., Cong, Z., and Wang, X.: Seasonal variation of secondary organic aerosol tracers in
664 Central Tibetan Plateau, *Atmos. Chem. Phys.*, 15, 8781-8793, 2015.
- 665 Surratt, J. D., Chan, A. W. H., Eddingsaas, N. C., Chan, M., Loza, C. L., Kwan, A. J., Hersey, S. P., Flagan, R.
666 C., Wennberg, P. O., and Seinfeld, J. H.: Reactive intermediates revealed in secondary organic aerosol
667 formation from isoprene, *Proc. Natl. Acad. Sci. U.S.A.*, 107, 6640-6645,
668 <https://doi.org/10.1073/pnas.0911114107>, 2010.
- 669 Tarvainen, V., Hakola, H., Hellén, H., Bäck, J., Hari, P., and Kulmala, M.: Temperature and light dependence of
670 the VOC emissions of Scots pine, *Atmos. Chem. Phys.*, 5, 989-998, 2005.
- 671 van der Werf, G. R., Randerson, J. T., Giglio, L., Collatz, G. J., Kasibhatla, P. S., and Arellano Jr, A. F.:
672 Interannual variability in global biomass burning emissions from 1997 to 2004, *Atmos. Chem. Phys.*, 6,
673 3423-3441, 2006.
- 674 Wang, F., Guo, Z., Lin, T., Hu, L., Chen, Y., and Zhu, Y.: Characterization of carbonaceous aerosols over the
675 East China Sea: The impact of the East Asian continental outflow, *Atmos. Environ.*, 110, 163-173,
676 <https://doi.org/10.1016/j.atmosenv.2015.03.059>, 2015.
- 677 Warneke, C., Froyd, K. D., Brioude, J., Bahreini, R., Brock, C. A., Cozic, J., de Gouw, J. A., Fahey, D. W.,
678 Ferrare, R., Holloway, J. S., Middlebrook, A. M., Miller, L., Montzka, S., Schwarz, J. P., Sodemann, H.,
679 Spackman, J. R., and Stohl, A.: An important contribution to springtime Arctic aerosol from biomass burning in
680 Russia, *Geophys. Res. Lett.*, 37, L01801, <https://doi.org/10.1029/2009GL041816>, 2010.
- 681 Yang, F., Gu, Z., Feng, J., Liu, X., and Yao, X.: Biogenic and anthropogenic sources of oxalate in PM_{2.5} in a
682 mega city, Shanghai, *Atmos. Res.*, 138, 356-363, <https://doi.org/10.1016/j.atmosres.2013.12.006>, 2014.
- 683 Yang, F., Kawamura, K., Chen, J., Ho, K., Lee, S., Gao, Y., Cui, L., Wang, T., and Fu, P.: Anthropogenic and
684 biogenic organic compounds in summertime fine aerosols (PM_{2.5}) in Beijing, China, *Atmos. Environ.*, 124,
685 166-175, 2016.
- 686 Zhang, H., Surratt, J. D., Lin, Y. H., Bapat, J., and Kamens, R. M.: Effect of relative humidity on SOA
687 formation from isoprene/NO photooxidation: enhancement of 2-methylglyceric acid and its corresponding
688 oligoesters under dry conditions, *Atmos. Chem. Phys.*, 11, 6411-6424,
689 <https://doi.org/10.5194/acp-11-6411-2011>, 2011.
- 690 Zhang, Q., He, K., and Huo, H.: Policy: cleaning China's air, *Nature*, 484, 161-162, 2012.
- 691 Zhang, Y., Yang, X., Brown, R., Yang, L., Morawska, L., Ristovski, Z., Fu, Q., and Huang, C.: Shipping
692 emissions and their impacts on air quality in China, *Sci. Total. Environ.*, 581-582, 186-198,
693 <https://doi.org/10.1016/j.scitotenv.2016.12.098>, 2017.
- 694 Zhang, Z., Zhang, Y., Wang, X., Lü, S., Huang, Z., Huang, X., Yang, W., Wang, Y., and Zhang, Q.:
695 Spatiotemporal patterns and source implications of aromatic hydrocarbons at six rural sites across China's
696 developed coastal regions, *J. Geophys. Res.-Atmos.*, 121, 6669-6687, <https://doi.org/10.1002/2016JD025115>,
697 2016.
- 698 Zhu, C., Kawamura, K., and Kunwar, B.: Effect of biomass burning over the western North Pacific Rim:
699 wintertime maxima of anhydrosugars in ambient aerosols from Okinawa, *Atmos. Chem. Phys.*, 15, 1959-1973,



- 700 <https://doi.org/10.5194/acp-15-1959-2015>, 2015.
- 701 Zhu, C., Kawamura, K., Fukuda, Y., Mochida, M., and Iwamoto, Y.: Fungal spores overwhelm biogenic organic
702 aerosols in a midlatitudinal forest, *Atmos. Chem. Phys.*, 16, 7497-7506, 2016a.
- 703 Zhu, C., Kawamura, K., and Fu, P.: Seasonal variations of biogenic secondary organic aerosol tracers in Cape
704 Hedo, Okinawa, *Atmos. Environ.*, 130, 113-119, <https://doi.org/10.1016/j.atmosenv.2015.08.069>, 2016b.
- 705 Zhu, Y., Yang, L., Kawamura, K., Chen, J., Ono, K., Wang, X., Xue, L., and Wang, W.: Contributions and
706 source identification of biogenic and anthropogenic hydrocarbons to secondary organic aerosols at Mt. Tai in
707 2014, *Environ. Pollut.*, 220, 863-872, 2017.
- 708 Zhu, Y., Li, K., Shen, Y., Gao, Y., Liu, X., Yu, Y., Gao, H., and Yao, X.: New particle formation in the marine
709 atmosphere during seven cruise campaigns, *Atmos. Chem. Phys.*, 19, 89-113,
710 <https://doi.org/10.5194/acp-19-89-2019>, 2019.